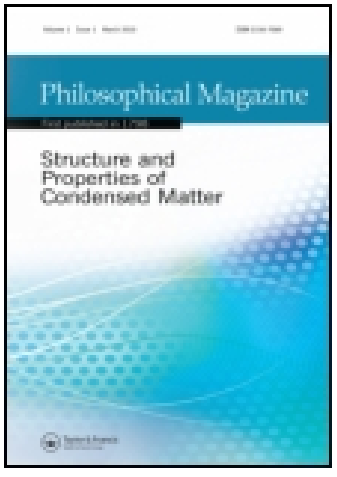

Philosophical Magazine
Publication details, including instructions for authors and subscription information:
http://www.tandfonline.com/loi/tphm20

Theoretical study on nanoindentation hardness measurement of a particle embedded in a matrix

Teck Fei Low[a], Chung Lun Pun[a] & Wenyi Yan[a]
[a] Department of Mechanical & Aerospace Engineering, Monash University, Clayton VIC 3800, Australia
Published online: 29 Apr 2015.

To cite this article: Teck Fei Low, Chung Lun Pun & Wenyi Yan (2015) Theoretical study on nanoindentation hardness measurement of a particle embedded in a matrix, Philosophical Magazine, 95:14, 1573-1586, DOI: 10.1080/14786435.2015.1040097

To link to this article: http://dx.doi.org/10.1080/14786435.2015.1040097

Philosophical Magazine, 2015
Vol. 95, No. 14, 1573–1586, http://dx.doi.org/10.1080/14786435.2015.1040097

Theoretical study on nanoindentation hardness measurement of a particle embedded in a matrix

Teck Fei Low, Chung Lun Pun and Wenyi Yan*

Department of Mechanical & Aerospace Engineering, Monash University, Clayton VIC 3800, Australia

(*Received 9 November 2014; accepted 1 April 2015*)

The finite element method was used to simulate indentation tests on a particle embedded in a matrix, to investigate the influence of the properties of the particle and the matrix, and the indentation depth on the measured hardness. The particle's work-hardening exponent and the mismatch in particle and matrix yield strength have a significant influence on the measured hardness. A particle-dominated indentation depth was identified, within which the measured nanoindentation hardness agrees very well with the true hardness of the particle material. Numerical results from the simulations of a wide range of material properties determined that the measured hardness is within 5% difference of the particle's true hardness when the indentation depth is less than 13.5% of the particle's radius. The results can be used in practice as a guideline to measure the hardness of a particle embedded in a matrix and provides the theoretical basis to develop a particle-embedded method to measure the hardness of individual particles.

Keywords: indentation; hardness; particle reinforced composite; particle-dominated depth; dimensional analysis; finite element analysis

1. Introduction

Nanoindentation test is an experimental method to probe the material properties of specimens, whereby a diamond indenter is usually pressed into the surface of a specimen with depths ranging in submicron scale. Its load-displacement data are recorded to extract material properties such as indentation hardness and Young's Modulus [1–7]. Nanoindentation tests have become a popular method to study the mechanical behaviour of small-sized materials, due to its simplicity and convenience.

In a particle-reinforced composite, nanoindentation on the particle could provide insight into the properties of the reinforcement [8–13]. Delincé et al. [14] conducted nanoindentation tests on both ferrite and martensite phases of dual phase steels to determine their strengthening contributions. Lee et al. [15] carried out nanoindentation tests on dendrite particles dispersed in Zr-based glassy matrix to determine its strengthening effects and ductility improvement. Melgarejo et al. [16] applied nanoindentation techniques to study the influence of aluminium diboride, AlB_2, particles on wear resistance of functionally-graded Al-AlB_2 composites.

*Corresponding author. Email: wenyi.yan@monash.edu

In a nanoindentation test on a particle embedded in a matrix, the matrix may influence particle measurements, which depends on the mismatch of particle and matrix material properties and the indentation depth relative to the size of particle [8–11]. Kashani et al. [12] studied the sizes of the volumes sampled by nanoindentation tests and found that for elastic-perfectly plastic materials, the intrinsic hardness of the particle can be measured as long as the plastic region is still within the particle while the zone influencing the Young's modulus is not restricted to a specific volume near the indenter. Durst et al. [8] studied dual-phase materials with different particle shapes using the finite element method and determined that particle hardness can be measured reliably, up to a normalised contact radius of approximately 70% particle radius. Yan et al. [9,10] found that the Oliver–Pharr method can still be used to measure the particle's Young's modulus with sufficient accuracy within a particle-dominated indentation depth. Leisen et al. [13] used continuous stiffness measurement to reduce the amount of error caused by using the Oliver–Pharr method to measure the Young's modulus of a particle embedded in a soft matrix.

The purpose of this research is to determine the influence of particle and matrix material properties on measured hardness from nanoindentation tests on a particle embedded in a matrix and establish a particle-dominated indentation depth for measuring the true hardness of the particle material. Research was carried out by parametric study and dimensional analysis with the aid of finite element modelling.

2. Investigation model and methodology

2.1. *Theoretical model*

Particle reinforced composites, or inclusions in inhomogeneous materials, were considered in this research. An idealized semi-spherical particle embedded in the surface of a semi-infinite matrix was investigated in this work, as shown in Figure 1. This model corresponds to a real situation of particles discretely distributed in a matrix with a relatively low particle volume fraction. In practice, a three-sided Berkovich indenter with face half-angle of 65.27° and a four-sided Vickers indenter with face half-angle of 68° are commonly used in commercial indentation instruments. Published study found that a conical indenter with half-angle of 70.3° can provide an equivalent projected contact area to the Vickers and Berkovich indenter [17]. Therefore, the conical indenter is

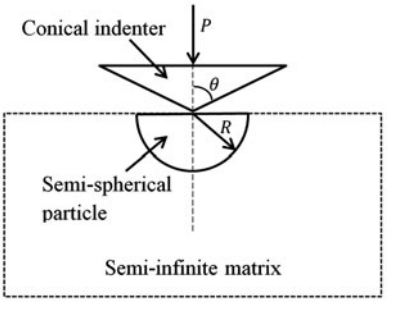

Figure 1. Schematic illustration of the indentation model.

normally applied to represent the Berkovich and the Vickers indenter in the axisymmetric finite element simulations for simplicity [17]. Sakharova et al. [18] and Kang et al. [19] investigated the influence of different indenter geometries with different face half-angle on the indentation responses and the measurement of mechanical properties of both bulk materials and composites. Although their studies indicate that the indentation responses from the conical indenter are not exactly the same as those from the Vickers and Berkovick indenters, the differences in the measured hardness are small. For instance, the hardness obtained from the conical indenter is only 5.1% and 6.3% less than that from the Vickers and the Berkovich indenters, respectively [19]. As the differences in the measured hardness are in an acceptable range, an axisymmetric conical indenter with half-angle of 70.3° was used in current study to simplify the finite element analysis. As illustrated in Figure 1, the conical indenter was pressed at the centre of the semi-spherical particle where P is the applied load and R is the radius of the particle. In this investigation, the radius of particle, R, is 4 μm.

In this research, the nanoindentation test was simulated by the finite element method via one cycle of loading and unloading using depth controlled indentation, whereby the indenter was pressed into the specimen until a specified indentation depth, h, was achieved. Research shows that the friction between the indenter and the specimen can influence the indentation responses, i.e. the maximum indentation force and the contact area, but the effects are relatively small in the case of Berkovich and Vickers indentations [20]. Our numerical results found that the maximum difference of the measured hardness is less than 10% with the friction coefficient varying from 0 to 0.5 when the normalized indentation depth is 12.5% of the particle's radius. Due to the difficulty in measuring the friction in practice and relatively small influence of friction on the indentation responses, frictionless contact between indenter and specimen was assumed in the simulations.

The indenter was assumed as a rigid body and it was constrained to vertical motion only. To validate this rigid indenter assumption, the numerical results confirm that the difference of the hardness values from an elastic diamond indenter and from a rigid indenter is less than 1% as long as the elastic modulus of the specimen is less than 65% of the elastic modulus of the diamond. The bottom of the specimen was constrained in both vertical and horizontal directions. In order to represent a semi-infinite body, the cylindrical matrix has a radius of 160 μm and depth of 160 μm. A numerical study was carried out to compare the numerical indentation curve of an elastic body with Sneddon's analytical solution [21] at different ratios of the indentation depth to the matrix radius (which is equal to the depth of the matrix). Our numerical results indicate that the error of the indentation force is less than 5% if the indentation depth is less than 1% of the matrix radius, which was used as the guide to determine the size of the matrix.

The commercial finite element package Abaqus was utilised to simulate the nanoindentation test using an axisymmetric model, which consists of 44,525 four-node axisymmetric elements (CAX4). Figure 2 illustrates the finite element model. The dimension of the fine-mesh region is 3.2 μm × 1.2 μm where the fine-mesh size is 10 nm × 10 nm. The mesh density was selected based on a convergence study to ensure that further refining the mesh will not affect the result. Additionally, this developed finite element model has been quantitatively and qualitatively validated by comparing

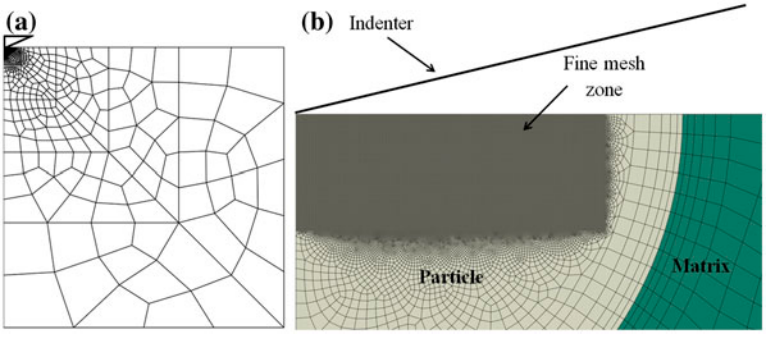

Figure 2. (colour online) Axisymmetric finite element model (a) model overview and (b) near particle-matrix boundary.

the numerical results of the indentation load-displacement responses with those provided in [8].

2.2. *Indentation hardness*

Hardness can be defined as a substance's resistance towards indentation [7,22,23], which can be quantified as:

$$H = P_{\max}/A, \tag{1}$$

where $P_{\max}$ is the maximum indentation load and A is the projected contact area of the indentation.

Current methods of obtaining the contact area from a nanoindentation test such as the Oliver–Pharr method is known to be unreliable for materials that exhibit significant pile-up deformation [3,5,7,24,25]. To avoid the influence of pile-up deformation on the hardness measurements, the contact area, A, was calculated based on the radius of contact, a_c, which was obtained from the finite element simulations. Since the finite element model is axisymmetric, the projected contact area, A, is given by:

$$A = \pi a_c^2. \tag{2}$$

Indentation hardness measured from the indentation test of a single-phase material with a sharp indenter is independent of indentation depth if the influence of indentation size effect is negligible. However, due to the dual-phase nature of the particle-matrix system studied here, matrix material properties could influence measurements obtained from nanoindentation tests on the particle [8–11]. To ensure the measured hardness is meaningful, it is essential to understand the influence of the mismatch in material properties between particle and matrix on the measured hardness and how this influence correlates with the indentation depth.

It is worth mentioning that hardness may decrease with the indentation depth for a crystalline material due to geometrically necessary dislocations in strain gradient plasticity at small indentation depths [26], which is known as indentation size effect. This indentation size effect is not considered in the study. It means that the findings can

be only applied to the particle materials without indentation size effect. In fact, it will lose the ground in practice to measure the hardness of a particle material if its hardness depends on the indentation depth.

3. Influence of material properties on measured hardness

The influence of the matrix on the measured hardness depends on the mismatch between the material properties of the particle and the matrix, and the indentation depth [7,8,24]. A parametric study to determine the influence of the material properties of a particle and its matrix on measured hardness was carried out via the finite element simulations.

Dimensional analysis is a useful tool for developing mathematical models for physical phenomena with the Buckingham Π-theorem [27]. The key feature of the dimensional analysis is to remove physical laws from its dependency of unit system [28]. Dimensional analysis has been successfully applied to analyse indentation response for different materials [8–11,24,29–32].

The measured indentation hardness, H, from a nanoindentation test of a particle embedded in a matrix depends on the mismatch in material properties of the particle and its matrix, geometry of the particle and the indenter, and the indentation depth. Taking into consideration that the indenter is conical and the particle is semi-spherical, the measured indentation hardness, H, is expressed as a function of all its independent parameters:

$$H = f(E_p, E_m, Y_p, Y_m, \nu_p, \nu_m, n_p, n_m, h_{\max}, \theta, R), \tag{3}$$

where E, Y, ν and n represent respectively the Young's modulus, initial yield strength, Poisson's ratio, and work-hardening exponent of the particle with subscript 'p' and the matrix with subscript 'm', $h_{\max}$ is the indentation depth at the maximum indentation load, $P_{\max}$, θ is the half-angle of the conical indenter, and R is the radius of the particle. Similar to single-phase materials [7], numerical results from current study indicates that the influence of ν_p and ν_m on the measured hardness is negligibly small. Therefore, Equation (3) can be rewritten as:

$$H = f(E_p, E_m, Y_p, Y_m, n_p, n_m, h_{\max}, \theta, R). \tag{4}$$

Applying Buckingham Π-theorem by using the basic physical quantities R and Y_p, the following dimensionless function can be obtained:

$$H/Y_p = \Pi(E_p/Y_p, E_m/Y_p, Y_m/Y_p, n_p, n_m, h_{\max}/R, \theta). \tag{5}$$

Data from the numerical simulations with $\theta = 70.3°$ and $\nu_p = \nu_m = 0.3$ were collected to analyse the relationship between H/Y_p and E_p/Y_p, E_m/Y_p, Y_m/Y_p, n_p, n_m and $h_{\max}/R$, which are detailed below.

Figure 3 shows the influence of the initial yield strength ratio of the matrix to the particle, Y_m/Y_p, on the measured hardness normalised with the particle yield strength, H/Y_p, for $0.1 \le Y_m/Y_p \le 5$. The influence of Y_m/Y_p on the measured hardness, H/Y_p, is large when $Y_m/Y_p < 1$ while it is small when $Y_m/Y_p > 1$. Results obtained shows that H/Y_p increases with Y_m/Y_p. However, this statement is not true for cases where $Y_m \ll Y_p$. As shown in Figure 3(a), H/Y_p increases with decreasing Y_m/Y_p for very small ratios of Y_m/Y_p.

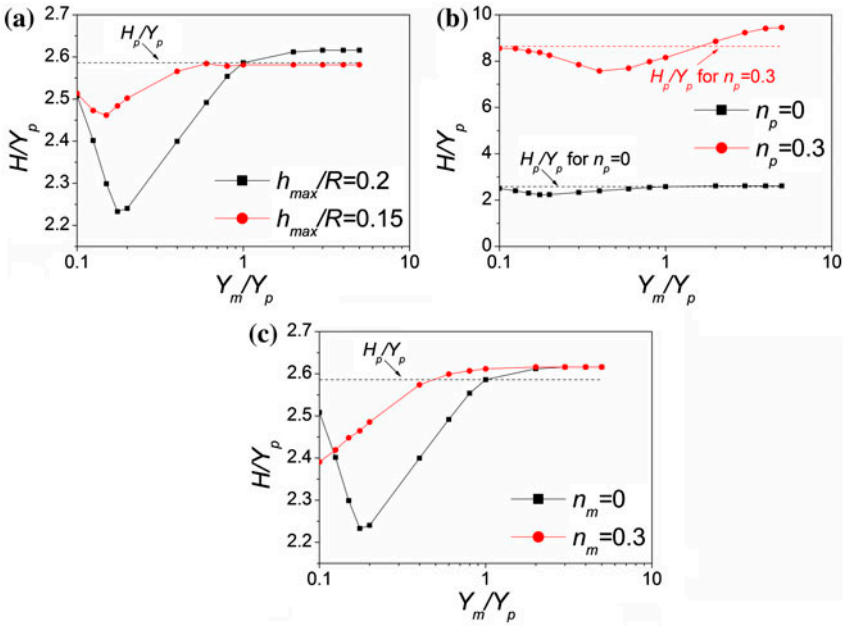

Figure 3. (colour online) Influence of Y_m/Y_p on H/Y_p when $E_p/Y_p = E_m/Y_p = 500$ where (a) $n_p = n_m = 0$, (b) $n_m = 0$ and $h_{max}/R = 0.2$, and (c) $n_p = 0$ and $h_{max}/R = 0.2$.

Additionally, H_p shown in Figure 3 represents the true hardness of the particle material, which can be measured from an indentation test of a bulk material with particle properties. H_p/Y_p is the ratio of particle's true hardness to its yield strength. Comparing the two curves in Figure 3(a), observations can be made on the influence of indentation depth on the measured hardness. The curve with a smaller normalised maximum indentation depth, h_{max}/R, has its normalised measured hardness, H/Y_p, closer to H_p/Y_p.

An observation can be obtained from Figure 3(b) and (c) when particle and matrix materials are work-hardened. Previous observations from Figure 3(a) indicate that H/Y_p increases with decreasing Y_m/Y_p when $Y_m/Y_p < 0.2$. In Figure 3(b) for $n_p = 0.3$, this phenomenon occurs when Y_m/Y_p is larger than 0.2. On the contrary, in Figure 3(c) for $n_m = 0.3$, this phenomenon does not occur even when $Y_m/Y_p = 0.1$. Based on Hollomon's equation [33], the relationship between yield strength and work-hardening exponent is given by:

$$Y = K\varepsilon_p^n, \tag{6}$$

where K is the strength index and ε_p is plastic strain. According to Equation (6), a larger work-hardening exponent will result in higher flow stress at a given plastic strain. In Figure 3(b), the hardness of particle compared to matrix would have been much larger due to work-hardening of the particle since the material's yield strength has a strong positive effect on its hardness. The opposite is true for Figure 3(c) due to work-hardening of the matrix. The greater mismatch in hardness in Figure 3(b) may have caused H/Y_p to increase with decreasing Y_m/Y_p much earlier compared to the

elastic-perfectly plastic examples. It can be concluded from Figure 3 that particle properties on the measured hardness are more dominant if the hardness of the particle is much greater than its matrix.

Figure 4 shows the influence of Young's moduli of the particle and the matrix on H/Y_p within the ranges of $10 \le E_p/Y_p \le 1000$ and $10 \le E_m/Y_p \le 1000$. Results obtained from Figure 4(a) shows that the influence of E_p/Y_p on H/Y_p is small when $E_p/Y_p > 70$. For $E_p/Y_p < 70$, H/Y_p decreases with decreasing E_p/Y_p. The nature of the curve is similar to a single-phase material with particle properties represented by H_p/Y_p in Figure 4(a). Cheng and Cheng found that for a single-phase material, H/Y approaches 1.7 when E/Y approaches 10 and H/Y is between 2.4 and 2.8 when $E/Y > 50$ [7]. This is consistent with the single-phase material results obtained in Figure 4(a) represented by H_p/Y_p.

In Figure 4(b), H/Y_p increases with increasing E_m/Y_p for $Y_m/Y_p = 1$ up to $E_m/Y_p = 200$. This is due to the influence of Young's modulus on hardness for small values of E/Y as shown by the H_p/Y_p curve in Figure 4(a). Measured hardness is smaller for small values of E_m/Y_p as the specimen behaves like a hard particle embedded in a soft matrix. Comparing results of $E_m/Y_p = 10$ and $E_m/Y_p = 200$, the difference in H/Y_p value obtained is 6.46%. For $Y_m/Y_p = 0.5$, the influence of E_m/Y_p on H/Y_p is also small. Change in E_m/Y_p from 10 to 1000 caused a maximum difference in measured hardness of 2.08%. Therefore, the influence of E_m/Y_p on hardness is not significant.

Figure 5 displays the influence of work-hardening exponent on measured hardness. Results in Figure 5(a) shows that increasing particle's work-hardening exponent increases measured hardness significantly. Also, the measured hardness is less when $h_{max}/R = 0.2$ compared to when $h_{max}/R = 0.15$. Since the hardness of the matrix is lower than the particle, a larger indentation depth increases the influence of matrix which results in a lower measured hardness. Figure 5(b) shows the relationship between n_m

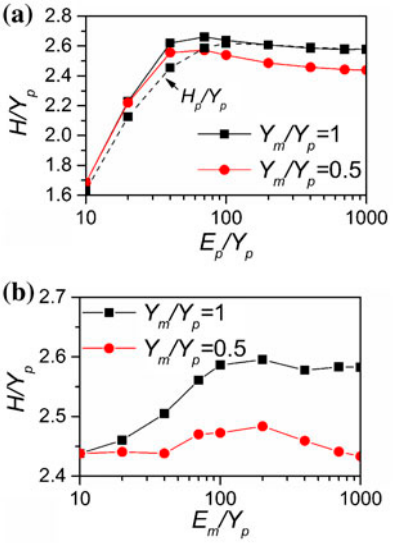

Figure 4. (colour online) Influence of Young's modulus on H/Y_p when $n_p = n_m = 0$ and $h_{max}/R = 0.2$ where (a) $E_m/Y_p = 500$ and (b) $E_p/Y_p = 500$.

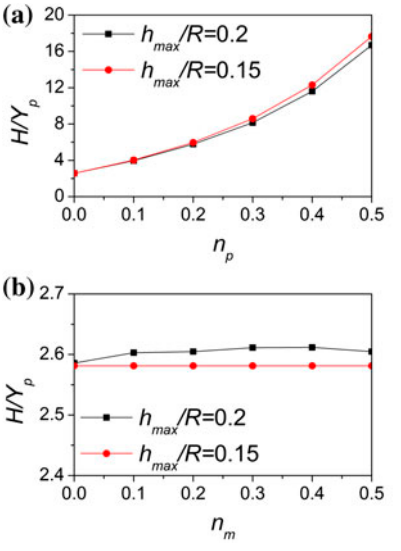

Figure 5. (colour online) Influence of work-hardening exponents on H/Y_p when $Y_m/Y_p = 1$ and $E_p/Y_p = E_m/Y_p = 500$ where (a) $n_m = 0$ and (b) $n_p = 0$.

and H/Y_p. It shows a negligible influence of the matrix's work-hardening exponent when $h_{max}/R = 0.15$. For $h_{max}/R = 0.2$, change in n_m from 0 to 0.5 causes a slight variation of measured hardness with the maximum difference of less than 2%. All the plots in Figure 5 have shown an increased influence of the matrix on the measured hardness when the indentation depth becomes larger.

4. Particle-dominated depth

Normalised particle-dominated depth, h_{pd}/R, is an indentation depth normalised with particle radius within which an indentation test to measure particle's true hardness is viable. For the purpose of determining the particle-dominated depth, there are 2 modes to be considered. The first mode is corresponding to the identification of a critical indentation depth over which the influence of matrix properties on measured hardness can no longer be considered negligible. Applying a tolerance error of 5%, the particle-dominated depth is the indentation depth at which measured indentation hardness normalised with particle's true hardness, H/H_p, is between 0.95 for a hard particle in a soft matrix and 1.05 for a soft particle in a hard matrix.

Figure 6 shows the relationship between normalised hardness, H/H_p, and normalised indentation depth, h/R, for two cases of nanoindentation tests on a particle embedded in a matrix. The first case is a hard particle ($Y_m/Y_p < 1$) embedded in a soft matrix, where $Y_m/Y_p = 0.2$, and the second case is a soft particle ($Y_m/Y_p > 1$) embedded in a hard matrix, where $Y_m/Y_p = 5$. The normalised particle-dominated depth, h_{pd}/R, is the point at which the normalised indentation depth, h/R, intersects $H/H_p = 0.95$ for hard particle or $H/H_p = 1.05$ for soft particle.

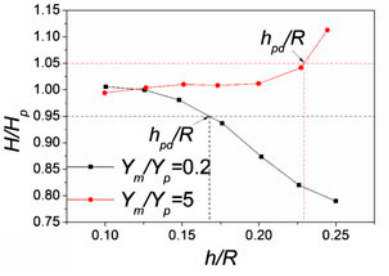

Figure 6. (colour online) Illustration of the method to determine the particle-dominated depth of a particle-matrix system where $E_p/Y_p = 100$, $E_m/Y_p = 2500$ and $n_p = n_m = 0$.

The second mode to be considered is the cases when the indenter establishes direct contact with matrix before the difference between the measured hardness and the particle's true hardness reaches to the maximum tolerance, see Figure 7. Numerical study indicates that these cases occur when particle's hardness is much greater than the hardness of the matrix and the presence of a large secondary indentation. Secondary indentation is defined as indentation of the matrix by the particle [11]. However, as direct contact is established, matrix properties will have a direct influence on measurements. In this mode, particle-dominated depth can be determined by the indentation depth at which the indenter starts to establish direct contact with the matrix.

In the example of Figure 7, the indentation depth, h, is 1.3 μm and the normalised hardness, H/H_p, is 0.957. Although the normalised hardness is between 0.95 and 1.05, increasing indentation depth would have caused the indenter and matrix to have direct contact causing the matrix to exert direct influence on measurements. Therefore, the normalised particle-dominated depth, h_{pd}/R is taken as 0.326 in this example.

The particle-dominated indentation depth, h_{pd}, depends on the material properties of the particle and its matrix, and the geometry of the particle and the indenter. Taking into consideration that the indenter is conical and the particle is semi-spherical, h_{pd} as a function of all its independent parameters is given by:

$$h_{pd} = f(E_p, E_m, Y_p, Y_m, v_p, v_m, n_p, n_m, \theta, R). \tag{7}$$

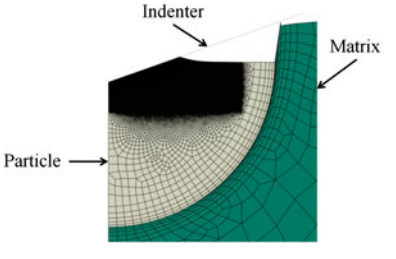

Figure 7. (colour online) An example of a second mode to determine the particle-dominated depth where $Y_m/Y_p = 0.1$, $E_p/Y_p = 2500$, $E_m/Y_p = 500$ and $n_p = n_m = 0$.

Numerical results indicate that the influence of v_p and v_m on the particle-dominated depth can be neglected. Equation (7) can be simplified as:

$$h_{pd} = f(E_p, E_m, Y_p, Y_m, n_p, n_m, \theta, R). \tag{8}$$

By applying Buckingham Π-theorem expressed in terms of R and Y_p, the following dimensionless function can be obtained:

$$h_{pd}/R = \Pi(E_p/Y_p, E_m/Y_p, Y_m/Y_p, n_p, n_m, \theta), \tag{9}$$

where θ was set constant at 70.3°. Data from numerical simulations were collected to analyse the relationship between h_{pd}/R and E_p/Y_p, E_m/Y_p, Y_m/Y_p, n_p and n_m. In the numerical simulations, Y_p was set constant at 200 MPa.

4.1. *Influence of work-hardening on particle-dominated depth*

Figure 8 displays the influence of work-hardening exponent on the relationship between normalised hardness, H/H_p, and normalised indentation depth, h/R, for cases of a hard particle embedded in a soft matrix. Figure 8(a) studies the influence of the particle's work-hardening exponent and Figure 8(b) studies the influence of the work-hardening exponent of the matrix. In both cases, results indicate that the $H/H_p \rightarrow 1$ when either of the work-hardening exponent increases. The implication of this observation is that for cases where $Y_m < Y_p$, the particle-dominated depth for measuring hardness for elastic-perfectly plastic particles (or matrices) is likely to be smaller than those with work-hardened particles (or matrices). The purpose of this study is to determine the minimum value of particle-dominated depth within which the measured hardness of a particle in a nanoindentation test of various particulate composites can be obtained. Therefore, the work-hardened particle and matrix can be discounted from the equation as it will give a

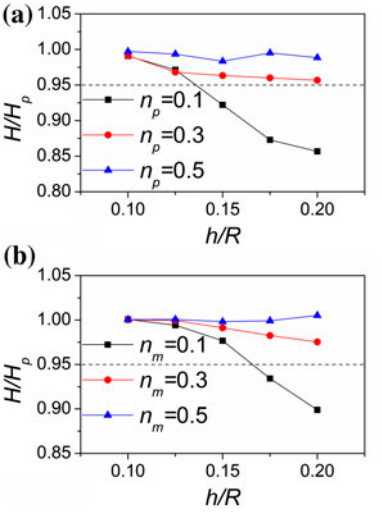

Figure 8. (colour online) Influence of work-hardening on the relationship between H/H_p and h/R when $Y_m/Y_p = 0.2$, $E_p/Y_p = 500$ and $E_m/Y_p = 1000$ where (a) $n_m = 0$ and (b) $n_p = 0$.

larger particle-dominated depth compared to those of elastic-perfectly plastic particles and matrices.

Figure 9 displays the influence of n_p on h_{pd}/R when $Y_m > Y_p$. For $Y_m/Y_p = 2$, the specimen behaves like a soft particle in a hard matrix when $n_p < 0.3$ and hard particle in soft matrix when $n_p > 0.3$. At $n_p = 0.3$, the measured hardness is very close to the true hardness of the particle even when h_{max}/R is larger than 0.25. For $Y_m/Y_p = 5$, the normalised particle-dominated depth reduces with n_p before reaching its lowest point at $n_p = 0.4$. When $n_p > 0.4$, the h_{pd}/R increases.

Shown in Figure 3(c), the difference between H_p/Y_p and H/Y_p for $n_m = 0.3$ when $Y_m > Y_p$ is very small with the maximum difference of 1.26%. Also shown in Figure 5(b), influence of n_m on measured hardness is small even when $h_{max}/R = 0.2$. Figure 9 has already established that the lower bound normalised particle-dominated depth is smaller than 0.2. Therefore, the influence of n_m can be neglected for cases where $Y_m > Y_p$ when determining the lower bound of particle-dominated depth to measure hardness of a particle embedded in a matrix.

4.2. *Influence of Young's modulus and yield strength on particle-dominated depth*

Figure 10(a) displays the influence of Y_m/Y_p on particle-dominated depth when $Y_m/Y_p < 1$ for different ratios of E_p/Y_p. The particle-dominated depth reduces with decreasing Y_m/Y_p until Y_m/Y_p is about 0.15. Further decreases of Y_m/Y_p would increase the particle-dominated depth. This minimum value is useful in establishing a guideline to conduct nanoindentation tests to measure hardness on a particle embedded in a matrix. Figure 10(b) displays the influence of Y_m/Y_p on particle-dominated depths when $Y_m/Y_p < 1$ for different ratios of E_m/Y_p. The particle-dominated depth reduces with decreasing Y_m/Y_p until Y_m/Y_p reaches a small value, which is about 0.2 for $E_m/Y_p = 100$ and about 0.125 for $E_m/Y_p = 2500$. Similar to Figure 10(a), further decreases of Y_m/Y_p would lead to an increase in the particle-dominated depth.

Results also revealed the occurrence of second mode of particle-dominated depth at $Y_m/Y_p = 0.1$ for $E_p/Y_p = 2500$ in Figure 10(a), $E_m/Y_p = 2500$ and $E_m/Y_p = 100$ in Figure 10(b). The second mode of particle-dominated depth is found to occur when $0.325 < h_{pd}/R < 0.334$. The purpose of investigating the particle-dominated depth for

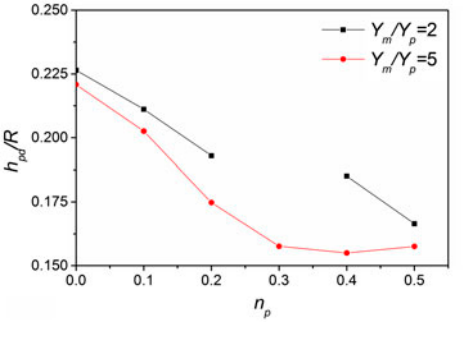

Figure 9. (colour online) Relationship between h_{pd}/R and n_p when $E_p/Y_p = 500$, $E_m/Y_p = 1000$, $v_p = v_m = 0.3$ and $n_m = 0$.

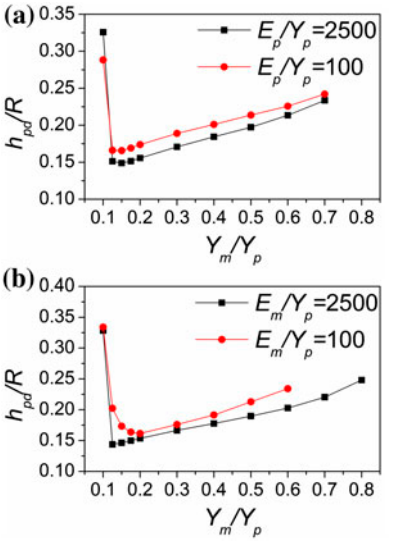

Figure 10. (colour online) Relationship between h_{pd}/R and Y_m/Y_p for cases of $Y_m/Y_p < 1$ when $v_p = v_m = 0.3$ and $n_m = n_p = 0$ where (a) $E_m/Y_p = 500$ and (b) $E_p/Y_p = 500$.

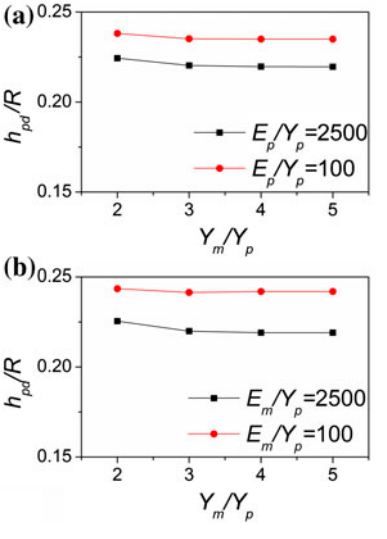

Figure 11. (colour online) Relationship between h_{pd}/R and Y_m/Y_p for cases of $Y_m/Y_p > 1$ when $v_p = v_m = 0.3$ and $n_m = n_p = 0$ where (a) $E_m/Y_p = 500$ and (b) $E_p/Y_p = 500$.

measuring hardness is to find a lower bound indentation depth at which indentation test on a particle embedded in a matrix can be carried out with certainty of obtaining the true hardness of the particle for a wide range of particle and matrix materials. For this

reason, the second mode of particle-dominated depth is less relevant as it occurs at larger indentation depths.

Figure 11 displays the relationship between particle-dominated depth and Y_m/Y_p for $2 \leq Y_m/Y_p \leq 5$. Results indicate that Y_m/Y_p has very little influence on particle-dominated depth when $Y_m/Y_p > 1$. However, both cases indicate that increase in E_p or E_m reduces the particle-dominated depth.

Comparing Figures 9–11, a normalised particle-dominated depth that serves as a guideline for carrying out nanoindentation tests can be established. It was found that for the case of an indentation on a semi-spherical particle embedded in a semi-infinite matrix, the minimum value for normalised particle-dominated depth, $h_{pd}/R = 0.135$. Provided that the indentation depth is less than 13.5% of the particle's radius, the measured hardness from a nanoindentation test on the particle would be within 5% of the particle's true hardness.

5. Conclusions

The finite element method was utilised to simulate nanoindentation tests on a semi-spherical particle embedded in the surface of a semi-infinite matrix. Dimensional analysis was applied to numerically analyse various combinations of particle and matrix material properties. Results revealed that particle's work-hardening exponent and the mismatch in the particle and matrix initial yield strength have a substantial influence on measured hardness. The influence of material property mismatch is dependent upon the indentation depth relative to the size of the particle. Also, for cases where the hardness of the particle is much larger than its matrix, particle properties are dominant when measuring hardness.

A particle-dominated depth whereby the hardness of a particle can be measured reliably from a nanoindentation test on the particle embedded in a matrix has been established in this research. Within this particle-dominated depth, the influence of matrix on particle measurements is negligible. The conclusion is based from a parametric study of an extensive range of particle and matrix material properties. Applying a tolerance level of 5%, whereby the measured hardness obtained from a nanoindentation test is within 5% of the actual hardness of the particle, it was found that the hardness of a particle can be measured reliably when the indentation depth is less than 13.5% of the particle's radius. This finding provides the guidelines to measure the hardness of a particle embedded in a matrix and it can also be applied as the basis to develop a particle-embedded method to measure the hardness of individual particles.

Disclosure statement

No potential conflict of interest was reported by the authors.

References

[1] J.L. Loubet, J.M. Georges, O. Marchesini and G. Meille, Tran. ASME J. Tribol. 106 (1984) p.106.
[2] M.F. Doerner and W.D. Nix, J. Mater. Res. 1 (1986) p.601.

[3] W.C. Oliver and G.M. Pharr, J. Mater. Res. 7 (1992) p.1564.
[4] K. Tunvisut, E.P. Busso, N.P. O'dowd and H.P. Brantner, Phil. Mag. A 82 (2002) p.2013.
[5] W.C. Oliver and G.M. Pharr, J. Mater. Res. 19 (2004) p.3.
[6] Z.H. Xu and J. Agren, Phil. Mag. 84 (2004) p.2367.
[7] Y.T. Cheng and C.M. Cheng, Mater. Sci. Eng. A R44 (2004) p.91.
[8] K. Durst, M. Göken and H. Vehoff, J. Mater. Res. 19 (2004) p.85.
[9] W. Yan, C.L. Pun and G.P. Simon, Compos. Sci. Technol. 72 (2012) p.1147.
[10] W. Yan, C.L. Pun, W. Wu and G.P. Simon, Compos. Part B 42 (2011) p.2093.
[11] J.W. Leggoe, J. Mater. Res. 19 (2004) p.2437.
[12] S.K. Kashani, A.A. Gilva and V. Madhavan, J. Mater. Res. 27 (2012) p.1553.
[13] D. Leisen, I. Kerkamm, E. Bohn and M. Kamlah, J. Mater. Res. 27 (2012) p.3073.
[14] M. Delincé, P.J. Jacques and T. Pardoen, Acta Mater. 54 (2006) p.3395.
[15] Y.H. Lee, J.S. Park, Y. Higo and D. Kwon, Mater. Sci. Eng. A 449–451 (2007) p.945.
[16] Z.H. Melgarejo, P.J. Resto, D.S. Stone and O.M. Suarez, Mater. Charact. 61 (2010) p.135.
[17] A.C. Fischer-Cripps, *Nanoindentation*, Springer, New York, 2002.
[18] N.A. Sakharova, J.V. Fernandes, J.M. Antunes and M.C. Oliveira, Int. J. Solids Struct. 46 (2009) p.1095.
[19] J.J. Kang, A.A. Becker and W. Sun, Appl. Mech. Mater. 70 (2011) p.219.
[20] J.L. Bucaille, S. Stauss, E. Felder and J. Michler, Acta Mater. 51 (2003) p.1663.
[21] I.N. Sneddon, Int. J. Eng. Sci. 3 (1965) p.47.
[22] H. O'Neill, *The Hardness of Metals and its Measurements*, Chapman and Hall, London, 1934.
[23] D. Tabor, Phil. Mag. A 74 (1996) p.1207.
[24] A.C. Fischer-Cripps, Surf. Coat. Tech. 200 (2006) p.4153.
[25] A. Bolshakov and G.M. Pharr, J. Mater. Res. 13 (1998) p.1049.
[26] W.D. Nix and H. Gao, J. Mech. Phys. Solids 46 (1998) p.411.
[27] E. Buckingham, Nature 96 (1915) p.396.
[28] T. Misic, M. Najdanovic-Lukic and L. Nesic, Eur. J. Phys. 31 (2010) p.893.
[29] M. Dao, N. Chollacoop, K.J. van Vliet, T.A. Venkatesh and S. Suresh, Acta Mater. 49 (2001) p.3899.
[30] W. Yan and C.L. Pun, Mater. Sci. Eng. A 527 (2010) p.3166.
[31] Q. Kan, W. Yan, G. Kang and Q. Sun, J. Mech. Phys. Solids 61 (2013) p.2015.
[32] Y.P. Cao, X.Y. Ji and X.Q. Feng, Philos. Mag. 90 (2010) p.1639.
[33] J.H. Hollomon, Trans. Am. Inst. Min. Metall. Pet. Eng. 162 (1945) p.268.